

28 sources and chemical oxygen demand-to-sulfate ratio ($\text{COD}/\text{SO}_4^{2-}$) on the diversity and
29 interactions of SRB and methanogens in an anaerobic digester treating a high-sulfate
30 waste stream. Overall, the data showed that sulfate removal and methane generation
31 occurred in varying efficiencies and the carbon source had limited effect on the
32 methane yield. Importantly, the results demonstrated that methanogenic and SRB
33 diversities were only affected by the carbon source and not by the $\text{COD}/\text{SO}_4^{2-}$ ratio.

34

35 Keywords: Anaerobic digestion, methanogens, sulfate reducers, COD/sulfate ratio

36

37 **1. INTRODUCTION**

38 Anaerobic digestion (AD) has been successfully deployed for decades to treat high-
39 strength industrial wastewaters and sewage sludge. Since methane, a renewable
40 energy source, is generated as the major end product, AD is considered the most
41 sustainable treatment process with a global primary energy potential of 99 EJ/year
42 projected for 2050 (Koornneef et al., 2013). However, the most recent estimates
43 indicate that currently only around 2.1 EJ/year is produced from the anaerobic
44 digestion of waste (WBA, 2014). Efficient AD process (from complex organic matter
45 degradation to biomethane generation) requires the concerted action of a well-
46 balanced microbial consortium composed of hydrolyzers, fermenters, syntrophic
47 microorganisms and methanogens. Despite numerous studies characterising these key
48 players, many unidentified microorganisms and unresolved metabolic pathways are
49 regularly observed in AD reactors, hence the AD process is still considered a 'black-
50 box' (Schmidt et al., 2016).

51

52 While many high-strength industrial wastewaters can be treated efficiently via
53 anaerobic digestion, anaerobic treatment of sulfate-containing wastewaters, such as
54 from the brewery, pulp and paper, food processing, and tannery industries, generates

55 very little methane. In sulfate-containing wastewaters terminal oxidation occurs via both
56 sulfate reduction and methanogenesis. Sulfate-reducing bacteria (SRB) use sulfate as
57 their terminal electron acceptor and can outcompete methanogenic archaea for carbon
58 and electrons (O'Flaherty et al., 1998). SRB may also compete with syntrophic bacteria
59 (e.g. acetogens) for short-chain volatile fatty acids such as propionate and butyrate
60 (Qatibi et al., 1990), while hydrogen sulfide production by SRB can inhibit both
61 methanogens and SRB (O'Reilly and Colleran, 2006). In addition to the competitive
62 interaction between methanogenic archaea and SRB, co-existence of methanogenesis
63 and sulfate reduction has been demonstrated in different ecosystems with high sulfate
64 concentrations such as estuarine sediments (Oremland and Polcin, 1982) and
65 anaerobic digesters (Isa et al., 1986). In environments with low sulfate concentrations,
66 H₂-utilising methanogens scavenge hydrogen produced during acidogenesis and
67 provide energetically favourable conditions for syntrophic SRB or acetogens (Parkin et
68 al., 1990; Muyzer and Stams, 2008; Bae et al., 2015). Moreover, the flexible
69 metabolism of many SRB increases their chance of survival in the absence of sulfate
70 (Plugge et al., 2011).

71

72 The interaction between methanogens and SRB is governed by several factors such as
73 the type and oxidation state of organic carbon as well as the carbon-to-sulfate ratio
74 (Bhattacharya et al., 1996; Raskin et al., 1996; Hu et al., 2015; Lu et al., 2016). For
75 instance, it has been shown that SRB in natural sediments prefer simple organic
76 compounds such as ethanol and acetate over more complex organic compounds and
77 usually outcompete methanogens if sulfate is available (Oremland and Polcin, 1982;
78 Pol et al., 1998). However, anaerobic metabolism in high-rate engineered systems
79 such as anaerobic digesters may differ significantly from natural sediments. In
80 anaerobic reactors treating sulfate-containing wastewaters, the carbon (measured as
81 chemical oxygen demand, COD) to sulfate ratio ($\text{COD}/\text{SO}_4^{2-}$) has been found to be

82 critical in determining the fate of the carbon; this ratio is usually kept above the
83 theoretical value of 0.67 to ensure complete sulfate removal. However, results from
84 previous research on the effect of COD/SO₄²⁻ are contradictory. For instance, methane
85 production from an upflow anaerobic sludge bed (UASB) reactor greatly deteriorated
86 when the COD/SO₄²⁻ ratio fell below 2 (Choi and Rim, 1991; Lu et al., 2016), whilst
87 other studies did not observe a significant effect of sulfate on methanogenesis (Hoeks
88 et al., 1984; Hu et al., 2015). The inconsistency between these observations may be
89 due to the differences in operational conditions such as wastewater characteristics and
90 reactor type used. Our knowledge of the diversity and metabolism of microorganisms in
91 AD reactors receiving sulfate-containing wastewaters is still very limited, which restricts
92 our understanding of these systems and hinders the development of strategies to
93 improve the methane production from AD reactors. In particular, sulfate may affect the
94 degradation pathway of carbon compounds present in the influent and of the
95 associated volatile fatty acids. Therefore, the effect of the COD/SO₄²⁻ ratio on the
96 interactions between SRB and methanogens as well as on the degradation pathway of
97 carbon compounds needs to be addressed.

98

99 In this study, we systematically evaluated the impact of three different COD/SO₄²⁻ ratios
100 and four different carbon sources on the methane yield and on the microbial population
101 dynamics in anaerobic sludge samples collected from a full-scale anaerobic digester
102 treating a sulfate-containing waste stream. Results revealed how the carbon source
103 and COD/SO₄²⁻ ratio affected the methane yield, the interactions between SRB and
104 methanogens and the metabolic pathways in anaerobic digester samples under
105 sulfidogenic conditions previously considered as unfavourable for methane generation.

106

107 **2. MATERIALS AND METHODS**

108 **2.1. Sample collection**

109 Anaerobic sludge samples were collected in July 2015 from three different sampling
110 ports of a UASB reactor of an industrial treatment plant that receives coffee production
111 wastewater (Jacobs Douwe Egberts Ltd, Banbury, UK), which contains sulfate. So, the
112 anaerobic sludge is acclimatised to sulfate. Samples were transferred to the laboratory
113 immediately and kept at 4°C until the experiments were set up.

114

115 **2.2. Potential methane production test**

116 A potential methane production (PMP) test was conducted to determine the optimum
117 concentrations and incubation times for four carbon sources (acetate, propionate,
118 butyrate and trimethylamine) to maximise methane production. Acetate, propionate and
119 butyrate were chosen as competitive, whilst trimethylamine (TMA) was chosen as a
120 non-competitive substrate for methanogens. Sludge samples from the three sampling
121 ports were mixed and washed twice in anaerobic medium with vitamin solution (DSMZ
122 318 and DSMZ 141, respectively; Braunschweig, Germany) to remove sulfate and
123 organic compounds from the samples. The washed sludge was centrifuged at 4000 *g*
124 for five minutes, the supernatant was decanted and the resulting pellet was
125 resuspended in equal volume of anaerobic medium as the removed supernatant.
126 Triplicate incubations were set up in 60 ml crimp-top serum bottles with 30 ml liquid
127 volume. Seed sludge with 1000 mg/l volatile suspended solids (VSS) was added to the
128 bottles. Acetate was tested at final concentrations of 10 to 60 mM, the other three
129 carbon sources were tested at 10 to 25 mM. The bottles were closed with butyl-rubber
130 stoppers and crimp-sealed with aluminium caps, flushed with oxygen-free nitrogen gas
131 for 10 min and then incubated at 35°C with shaking (150 rpm, Innova 4300, New
132 Brunswick Scientific Ltd., UK). Headspace gas pressure was measured daily using a
133 handheld digital manometer (Dwyer Series 475, Dwyer Instruments Ltd, UK) and the
134 incubations were ceased once gas production stopped.

135

136 PMP test results showed that the highest methane productions were obtained when
137 the samples were incubated with 45 mM acetate, 20 mM propionate, 15 mM butyrate
138 and 15 mM trimethylamine (Supplementary Figure 1). Incubations with acetate,
139 propionate and butyrate reached the highest PMP on day seven whilst TMA
140 incubations took 12 days. Therefore, experiments were set up using these
141 concentrations and incubated for seven (acetate, propionate and butyrate) or 12 days
142 (TMA) to provide conditions for maximum methane production and avoid substrate
143 inhibition.

144

145 **2.3. Experimental design**

146 Batch experiments were used to assess the impact on methane yield of acetate,
147 propionate, butyrate and TMA at three different COD/SO₄²⁻ ratios (0.5, 1.5 and 5) and to
148 analyse interactions between anaerobic microbial populations. No-sulfate incubations
149 were set up as controls. Five replicated microcosms were prepared for each substrate
150 and COD/SO₄²⁻ combination using inoculum adjusted to 1000 mg/l VSS in 60 ml serum
151 bottles with 30 ml liquid volume. Guided by the PMP test, different carbon (15, 20 or 45
152 mM) and sulfate (1.5 – 66.7 mM) concentrations were provided to establish the
153 selected COD/SO₄²⁻ ratios (Supplementary Table 1). The microcosms were run for
154 seven (acetate, butyrate and propionate) or 12 days (TMA).

155

156 **2.4. Methane and volatile fatty acids analysis**

157 At the end of the incubations, gas samples were collected using a gas-tight syringe
158 (Hamilton Company, Reno, USA) and the methane production was monitored by gas
159 chromatography (Agilent 6890N, Agilent Technologies, Cheshire, UK) fitted with a
160 flame ionisation detector and Porapak Q column. Nitrogen with 20 ml/min was used as
161 the carrier gas. Three measurements were taken for each microcosm and the mean
162 was calculated.

163

164 Slurry samples were also collected at the end of the incubations and centrifuged at
165 4000 *g* for five minutes. Supernatant was collected, filtered through a 0.20 μm
166 polyethersulfone membrane and analysed for volatile fatty acids (VFA) and sulfate
167 using an ion exchange chromatography (Dionex ICS3000; Dionex Corp., Sunnyvale,
168 CA, USA). Anion analysis was done using an Ionpac AS 18 column (2 mm x 50 mm)
169 equipped with an Ionpac AS 18 guard column, while cation analysis was done using an
170 Ionpac CS12A column (4 mm x 250 mm) equipped with an Ionpac CG12A guard
171 column. A gradient of 0-30 mM KOH and 20 mM methylsulfonic acid was used as
172 eluent for anion and cation analyses, respectively.

173

174 **2.5. Molecular methods**

175 *2.5.1. DNA extraction and PCR*

176 Three replicates (out of five) that had less than 5% difference in methane generation
177 from each treatment and controls were chosen for molecular analysis. Slurry samples
178 were collected as above and total genomic DNA was extracted from 500 mg of
179 centrifuged slurry from each selected incubation using the hydroxyapatite spin-column
180 method (Purdy, 2005). Bacterial and archaeal 16S rRNA genes and functional genes
181 specific to methanogens (methyl coenzyme M reductase, *mcrA*) and SRB (dissimilatory
182 sulfate reductase, *dsrB*) were amplified by PCR (Supplementary Table 2). All PCR
183 amplifications were carried out using a Mastercycler Pro thermal cycler (Eppendorf UK
184 Ltd., Stevenage, UK) with MyTaq Red DNA Polymerase (Bioline Reagents Ltd.,
185 London, UK). Amplification conditions for the 16S rRNA and the *mcrA* genes were as
186 follows: initial denaturation at 95°C for 5 min, 35 cycles of 95°C for 1min, 55°C for 1
187 min, 72°C for 1.5 min, a final elongation step at 72°C for 5 min. For the *dsrB* gene, the
188 PCR conditions were the same except the annealing temperature, which was 52°C.

189

190 *2.5.2. High-throughput sequencing and data analysis*

191 16S rRNA and functional gene PCR products were sequenced on the Illumina MiSeq
192 platform (300 bp paired-end, Illumina, Inc, San Diego, CA, USA) at the University of
193 Warwick (UK). Before sequencing, the PCR products were cleaned using Charge
194 Switch PCR Clean-up kit (Invitrogen, CA, USA), quantified by Qubit dsDNA BR Assay
195 Kit with Qubit 2.0 Fluorometer (Invitrogen, CA, USA), and prepared for sequencing as
196 described by Caporaso et al. (2012).

197

198 We obtained 4.7, 3.3, 8.6 and 7.5 Gb raw sequences for the *mcrA*, *dsrB*, bacterial and
199 archaeal 16S rRNA genes, respectively. Raw sequences were quality-trimmed using
200 Trimmomatic (Bolger et al., 2014). Merging and operational taxonomic unit (OTU)
201 picking were carried out by USEARCH v8 (Edgar, 2010) at 97% and 85% similarity cut-
202 off for the 16S rRNA and the functional gene sequences, respectively. Chimeras were
203 checked using ChimeraSlayer (Haas et al., 2011) and removed from downstream
204 analysis. Taxonomy assignments were determined against the Greengenes database
205 (DeSantis et al., 2006) for bacteria and archaea, and custom *dsrB* and *mcrA* databases
206 (Müller et al., 2015; Wilkins et al., 2015) using RDP Classifier 2.2 (Wang et al., 2007)
207 via QIIME software, version 1.6.0 (Caporaso et al., 2010). Average relative abundance
208 for each OTU in the samples was calculated using the relative OTU read abundances
209 of three replicates. Sequence datasets have been submitted to the National Center for
210 Biotechnology Information (NCBI) Read Archive under the bioproject accession
211 number of PRJNA434657.

212

213 2.5.3. Quantitative PCR (qPCR)

214 In order to relate the methane generation to the relative abundance of methanogens,
215 total *mcrA* gene copies in the incubation bottles were quantified using a qPCR assay
216 with the *mcrA*-specific PCR primers (Supplementary Table 2). A standard curve was
217 produced using serial 10-fold dilutions of a plasmid containing the *mcrA* gene. PCR
218 reaction volumes were 10 ul, comprising 2 ul of 1:10 diluted gDNA, 0.35 ul of each

219 primer, 2.3 ul H₂O and 5 ul SsoAdvanced Universal SYBR Green Supermix (Bio-Rad
220 Laboratories Ltd., Hertfordshire, UK). Samples were run on a Bio-Rad CFX Connect
221 Real-Time Detection System (Bio-Rad Laboratories Ltd., Hertfordshire, UK). The
222 cycling conditions were as follows: 98 °C for 3 min, followed by 40 cycles of 98 °C for
223 15 s, 55 °C for 15 s, 72 °C for 1 min. To check for non-specific DNA products, a melt
224 curve was performed by heating the reaction mixture from 65 to 95°C with 0.5°C
225 increments. The efficiency of the reactions was between 103%-109%, while the R²
226 value for the standard curve was 96%.

227

228 **2.6. Statistical analysis**

229 One-way ANOVA with Post-hoc Dunnett's test was conducted to determine the
230 statistical significance of difference in biomethane production in the microcosms.
231 Species richness (Chao1) and alpha diversity (Shannon's index) were calculated using
232 OTU numbers and relative abundances. Principal Components Analysis (PCA) was
233 also applied to the relative abundance of OTUs to discriminate the samples with
234 respect to treatments. Following this, Spearman's correlation analysis was carried out
235 to identify the factors that may have affected the OTU abundances by correlating the
236 first two principal components to the experimental variables including the methane
237 generation, sulfate removal efficiency, COD/SO₄²⁻ ratio as well as the concentrations of
238 sulfate and the carbon compound removed. Graphpad Prism 7 software (Graphpad
239 Software, CA, USA) was used for correlation analysis and one-way ANOVA test, while
240 PAST (version 3) was used for diversity indices and PCA (Hammer et al., 2001).

241

242 **3. RESULTS AND DISCUSSION**

243 **3.1. Methane production and sulfate reduction efficiencies under different**

244 **COD/SO₄²⁻ ratios**

245 Methane, VFA and sulfate concentrations in the microcosms were measured at the end
246 of the incubation and mass balances were calculated (Table 1). Results showed that
247 three carbon sources (acetate, propionate and butyrate), and any VFAs produced as
248 by-products, were consumed during the incubation period (data not shown). However,
249 ~30% of the added TMA (123 to 137 μ moles) was not consumed in the incubation time.

250

251 The methane production and sulfate reduction for each substrate were assessed by
252 comparison to the no-sulfate control microcosms. Methane production was also
253 compared to the theoretical methane yields based on the amount of substrate utilised
254 (Bushwell and Mueller, 1952). Both acetate- and propionate-amended microcosms
255 produced methane in amounts close to their theoretical maximum (1350 μ moles and
256 1050 μ moles, respectively, Figure 1a, Table 1), while butyrate- and TMA-amended
257 microcosms produced no more than 60% of their theoretical maximum (1500 μ moles
258 and 704-734 μ moles, respectively, Figure 1a, Table 1).

259

260 In acetate-amended microcosms, there was no significant difference between the
261 methane generation in controls and sulfate-amended microcosms. Similarly, in a
262 previous study, an anaerobic sludge sample, acclimated to sulfate-rich pulp and paper
263 wastewater, utilized 2000 mg/L acetate and produced 700 mL methane, which was
264 approximately the theoretical maximum (Ince et al., 2007). On the other hand,
265 propionate and TMA had lower methane yields when COD/SO₄²⁻ ratio was 0.5 and 1.5
266 compared to the controls, while butyrate-amended samples with all COD/SO₄²⁻ ratios
267 had lower methane yields compared to the controls. It should be noted that hydrogen
268 sulfide (H₂S) produced by the reduction of sulfate might have an inhibitory effect on
269 some methanogenic species, which might lower the methane generation (Isa et al.,
270 1986). However, we used sulfate-acclimated anaerobic sludge to set up the
271 experiments, so the inhibitory effect of H₂S would likely be reduced in our microcosms.

272 This may be the reason why we did not observe any significant drop in methane
273 generation from acetate-amended microcosms with or without sulfate. Furthermore,
274 there is experimental evidence that the kinetic and thermodynamic advantages of sulfate
275 reducers over methanogens are erased by their sensitivity to sulfide toxicity, which may
276 explain the methanogenic activity observed in our microcosms amended with sulfate
277 (Maillacheruvu and Parkin, 1996).

278

279 The effect of COD/SO₄²⁻ ratio on methane generation and sulfate removal in the
280 microcosms was limited, and depended on the carbon source utilised. There was no
281 significant effect of changing the COD/SO₄²⁻ ratio on the methane production in the
282 acetate-, butyrate- and TMA-amended samples (Figure 1a, p>0.05). There was a
283 small, but significant (p<0.01) decrease in methane production in propionate-amended
284 samples at a COD/SO₄²⁻ ratio of 1.5. However, even within these microcosms there was
285 no pattern of decreasing methane production with increasing sulfate. The consistent
286 methane production with an increasing COD/SO₄²⁻ ratio suggests that sulfate reduction
287 does not affect methanogenesis in either the acetate- or propionate-amended
288 microcosms. This is despite the fact that, in other systems, both of these substrates are
289 preferentially utilised by SRB if sulfate is freely available (Purdy et al., 2003a, 2003b)
290 and acetate-based sulfate reduction is more thermodynamically favourable than
291 acetoclastic methanogenesis (Schönheit et al., 1982).

292

293 Methane production in the butyrate- and TMA-amended microcosms was between
294 44% - 82% of their theoretical maximum (Figure 1a, Table 1) in all treatments and
295 significantly lower than the no-sulfate controls in all samples. However, there was no
296 significant difference in methane production across the three COD/SO₄²⁻ ratios for both
297 substrates, which suggests that the presence but not the concentration of sulfate
298 affected the methane production. The limited methane production with butyrate and

299 TMA indicates that non-methanogenic pathways for both butyrate and TMA
300 degradation occurred in these incubations.
301
302 Sulfate removal efficiency increased with increasing COD/SO₄²⁻ ratio in all four
303 treatments (Figure 1b, Table 1) with only the acetate-amended microcosms not
304 reaching ~100% removal of sulfate (maximum of 70% removal). The effect of sulfate
305 addition on methane production in TMA-amended microcosms is remarkable, as this
306 compound is not known to be a competitive substrate for SRB. Hence, our results
307 disagree with those of Vich et al (2011), who amended methylamine and sulfate to
308 sludge samples from a full-scale UASB reactor and observed no significant effect of
309 sulfate addition on methane generation. In the propionate-amended samples at 0.5
310 and 1.5 COD/SO₄²⁻ ratios, available sulfate had a small but statistically significant effect
311 on methane production (p<0.01; Figures 1a and 1b). Our results contradict two recent
312 studies, where the effect COD/SO₄²⁻ ratio on methane generation was investigated. In a
313 study by Lu et al. (2016) on the effect of influent COD/SO₄²⁻ ratio on the biodegradation
314 of starch wastewater in a lab-scale UASB reactor, sulfate addition enhanced
315 sulfidogenesis and subsequently methanogenesis. However, when the COD/SO₄²⁻ ratio
316 was lower than 2, methanogenesis was suppressed, possibly due to the competition and
317 H₂S inhibition (Lu et al., 2016). Similarly, Kiyuna et al. (2017) found that high sulfate
318 concentrations significantly reduced methane production from sugarcane vinasse,
319 however these authors used higher COD/SO₄²⁻ ratios (7.5, 10 and 12) than we used in
320 our study.

321
322 While our results showed that methane production and sulfate reduction are
323 independent pathways for readily biodegradable substrates, in full-scale applications,
324 both COD removal efficiency and methane production in anaerobic treatment of
325 complex, sulfate-rich wastewaters may be lower. This may be due to the low

326 biodegradability of wastewater and the inhibitory effect of high sulfate/sulfur
327 concentration on microbial activity (Lens et al., 1998).

328

329 **3.2. Taxonomic and functional diversities in the microcosms**

330 Between 1.7 and 3.8 million quality-filtered, chimera-free sequences were obtained for
331 bacterial 16S rRNA, archaeal 16S rRNA, *dsrB* and *mcrA* genes. These sequences
332 were assigned to 1295 and 543 distinct OTUs at 97% identity for bacterial and
333 archaeal 16S rRNA genes, whilst 288 and 61 distinct OTUs were obtained at 85%
334 identity for *dsrB* and *mcrA* genes, respectively. There was no significant difference
335 between the observed and predicted numbers of OTUs for each marker gene within
336 each treatment as estimated by Chao1 (Supplementary Table 3). The Shannon
337 diversity index did not vary significantly across samples (Supplementary Table 3).

338

339 We observed distinct shifts in the specific microbial populations in the microcosms over
340 the experimental period, which allowed us to draw conclusions about the impact of
341 carbon sources and the COD/SO₄²⁻ ratio on the diversity and metabolic interactions of
342 SRB and methanogens.

343

344 *3.2.1. Methanogenic diversity and abundance*

345 *Methanobacterium* spp, which use H₂ and CO₂ to produce methane (Boone, 2001),
346 dominated the methanogenic communities in all incubations (67-82% of the *mcrA*
347 sequences, Figure 2a). This finding was confirmed by archaeal 16S rRNA sequencing
348 (Figure 3a). The strong dominance of hydrogenotrophic methanogens even in the
349 presence of sulfate demonstrates that H₂-consuming methanogens were not
350 outcompeted by H₂-consuming SRB, which has been suggested to be a characteristic
351 of nutritious, high-rate systems such as anaerobic digesters (Ueki et al., 1992). The
352 consistently low percentage of *Methanosaeta* sequences (0.1-0.7%) in all the

353 microcosms indicates that acetoclastic methanogenesis was not a significant process
354 in this bioreactor (Demirel and Scherer, 2008). This is clearly shown in the fact that
355 even the addition of acetate did not enhance *Methanosaeta* (Figure 2a), suggesting
356 acetoclastic methanogenesis was not active at all in these slurries, despite the fact that
357 100% of the predicted methane was produced in the acetate-amended samples
358 (Figure 1a).

359

360 In the TMA-amended microcosms, the methanogenic community structure shifted. In
361 these incubations, the relative abundance of the obligate methylotrophic genus
362 *Methanomethylovorans* (Lomans et al., 1999) increased significantly to 20.1% ($\pm 1.8\%$,
363 $p=0.003$) from 1% in the other incubations, irrespective of the COD/SO₄²⁻ ratio (Figure
364 2a). Methylotrophic methanogens dominate TMA degradation in marine sediments
365 (King, 1984; Purdy et al., 2003a), so it is not unexpected that sulfate reduction and
366 methanogenesis were independent in TMA-amended microcosms and the relative
367 abundance of *Methanomethylovorans* was not affected by the presence or the
368 concentration of sulfate (Figure 2a). PCA analysis of the *mcrA* sequences also
369 supported this finding, as it separated the TMA incubations from the rest of the
370 samples (Figure 2b). The first principal components explained 82% and 84% of the
371 total variability in the *mcrA* (Figure 2b) and archaeal diversities (Figure 3b) in the
372 samples, respectively.

373

374 In addition to the sequence analysis, we have also quantified the *mcrA* genes to reveal
375 the abundance of the methanogens in the samples. The *mcrA* gene numbers
376 increased about ten-fold, from about 1.1×10^5 to about 1.6×10^6 across all microcosms
377 (Supplementary Figure 2). The pattern was different for different substrates, though.
378 The average abundance of the methanogens increased from 2.3×10^5 to 1.6×10^6 in the
379 acetate-amended microcosms as the COD/SO₄²⁻ ratio increased, however this increase

380 was not statistically significant. There was also no statistically significant difference in
381 the methanogen abundance in propionate-amended microcosms, in spite of an
382 increase in methane production at the highest COD/SO₄²⁻ ratio. This suggests an
383 increase in the specific methanogenic activity in these microcosms. The lowest
384 methanogen abundance was observed in the butyrate-amended microcosms, which
385 was consistent with the methane production in these incubations, where the methane
386 yield was lower than the other microcosms (Figure 1). The number of methanogens did
387 not change significantly in the TMA-amended microcosms and they had a similar
388 number of methanogens to acetate and propionate incubations although the methane
389 yield was lower. This might be due to the lower efficiency of *Methanomethylovorans*
390 spp in utilising TMA compared to hydrogenotrophic methanogens dominating other
391 incubations.

392

393 Correlation analyses revealed that the *mcrA* and archaeal diversities did not
394 significantly correlate with the COD/SO₄²⁻ ratio in the microcosms, while the first
395 principal component of the *mcrA* analysis significantly correlated with only the methane
396 yield (p <0.01; Figure 2b and 3b; Table 2). Methanogen abundance did not correlate
397 significantly with the methane yield in the microcosms, however sulfate removed was
398 significantly related to the archaeal diversity (Table 2).

399

400 3.2.2. SRB diversity

401 The SRB diversity, as determined by sequencing the *dsrB* gene, did not change
402 markedly with the COD/SO₄²⁻ ratio in the microcosms (Figure 4a). This counterintuitive
403 result could be explained by the metabolic flexibility of SRB, which allows some of
404 them act as fermenters when sulfate is not available (Plugge et al., 2011). Some SRB
405 can form syntrophic associations with H₂ scavengers such as hydrogenotrophic
406 methanogens, utilising the H₂ produced by SRB (Bryant et al., 1967; Stams and

407 Plugge, 2009). Indeed, hydrogenotrophic methanogenesis was the dominant
408 methanogenic pathway in the microcosms, which might enable SRB survival in the
409 sulfate-free control incubations.
410
411 The relative mean read abundance of the *Desulfarculus baarsii* lineage increased from
412 ~6% to 14%-23.5% in the butyrate-amended microcosms (Figure 4a). *Desulfarculus*
413 *baarsii* can oxidise acetate and fatty acids completely to CO₂ using sulfate as an
414 electron acceptor (Sun et al., 2010). Although they have not been shown to grow
415 without sulfate in syntrophy with methanogens to date (Muyzer and Stams, 2008;
416 Plugge et al., 2011), they were found in the control incubations without added sulfate.
417 However, presence does not mean activity: these *D. baarsii* species may have been
418 present but inactive in the control incubations without sulfate. PCA analysis of the *dsrB*
419 sequence data revealed that the first component accounted for 97.9% of the total
420 variability, separating the butyrate incubations from the rest of the samples (Figure 4b).
421 Interestingly, there was no significant correlation between the *mcrA* and *dsrB*
422 diversities, and with the COD/SO₄²⁻ ratio (Table 2), which further indicates that methane
423 production and sulfate reduction were independent processes in these samples.
424 However, the *dsrB* diversity was found to be correlated with the concentration of sulfate
425 removed, sulfate removal efficiency, the initial carbon concentration and the methane
426 yield (Table 2).

427

428 3.2.3. Bacterial Diversity

429 The most striking result from the bacterial sequence analysis was the dramatic
430 increase in the relative abundance of the genus *Syntrophomonas* in the butyrate
431 incubations to 8.9%± 1.02% from 1.1% ± 0.3% in the other microcosms (p=0.003,
432 Figure 5a). As in the *mcrA* and *dsrB* diversities, this change was not dependent on the
433 COD/SO₄²⁻ ratio (Figure 5a and 5b). *Syntrophomonas* species can degrade butyrate to

434 acetate and H₂ (Schmidt et al., 2013), and have been shown to form syntrophic
435 interactions with hydrogenotrophic *Methanobacterium* spp (Sousa et al., 2007). We
436 suggest that the members of this genus worked in syntrophy with *Methanobacterium*
437 spp., which utilised H₂ to produce methane, particularly in the butyrate-amended
438 microcosms. Similar cooperation was observed in co-cultures of *Syntrophomonas*
439 *wolfei* and *Methanospirillum hungatei*, which coupled butyrate degradation to acetate
440 and H₂ formation during growth on butyrate (Schmidt et al., 2013).

441

442 All the microcosms, including the controls, consistently contained *Syntrophobacter* in
443 relatively high abundances (3.6-7%). This is in line with a previous research, showing
444 that *Syntrophobacteriales* are a stable and resilient functional group of bacteria in
445 anaerobic digestion systems (Werner et al., 2011). *Syntrophobacter* species can grow
446 on acetate, propionate and butyrate, either by sulfate reduction or, in the absence of
447 sulfate, by fermentation in syntrophy with methanogens and other H₂/formate oxidisers
448 (Sobieraj and Boone, 2006; Müller et al., 2010, 2013) . Their metabolic flexibility may
449 explain their high relative abundance across the samples regardless of the carbon
450 compound or the COD/SO₄²⁻ ratio used (Boone and Bryant, 1980; Muyzer and Stams,
451 2008; Plugge et al., 2011).

452

453 Bacterial diversity significantly correlated only with methane production (p <0.05, Table
454 2), which may be due to the effect of the carbon sources on the bacterial populations,
455 as clearly observed in the butyrate set. There was no significant correlation between
456 bacterial diversity and COD/SO₄²⁻ ratio across the samples (Table 2).

457

458 **3.3. Metabolic interactions between the microbial communities**

459 Sulfate reduction and methane generation were observed in varying efficiencies in the
460 microcosms, whilst the relative abundances of specific functional groups such as

461 syntrophic organisms and hydrogenotrophic or methylotrophic methanogens
462 (*Methanobacterium* spp and *Methanomethylovorans* spp.) did not vary considerably
463 within each set despite the change in the COD/SO₄²⁻ ratio (Figure 2-5). This may be
464 explained by the flexible metabolism of SRB, which allows these populations to survive
465 when there is no available sulfate to respire as discussed above for *D.baarsii*.
466 Furthermore, syntrophic associations between methanogens and SRB may have
467 facilitated their growth together, as was previously shown in sulfate-amended
468 anaerobic reactors, which had high sulfate-reduction efficiency even when
469 hydrogenotrophic methanogens were dominant (Yang et al., 2015).

470

471 We derived metabolic pathways for the metabolism of the carbon compounds used in
472 this study based on the dominant microbial populations as obtained by the sequence
473 analysis. In acetate amended microcosms, efficient methane generation was observed
474 with and without sulfate and there was no marked change in microbial diversity under
475 different COD/SO₄²⁻ ratios. According to the sequence analysis, different metabolic
476 pathways for the mineralization of acetate could be active simultaneously in these
477 microcosms, independent of the COD/SO₄²⁻ ratio (Figure 6a).

478

479 *Desulfarculus baarsii* species can convert acetate to CO₂, which can be further used to
480 produce methane. Similarly, syntrophic acetate oxidation coupled to hydrogenotrophic
481 methanogenesis, which is thermodynamically and physiologically feasible at mesophilic
482 temperatures, may have occurred efficiently in these microcosms (Schnürer and
483 Nordberg, 2008; Dolfing, 2014). We propose that methane generation from propionate
484 was via similar pathways (Figure 6b), with propionate being converted to acetate first
485 as it is not utilised by methanogens directly. The dominance of the members of the
486 *Desulfarculus baarsii* lineage and the genus *Syntrophobacter* suggests complete
487 oxidation of propionate to H₂+CO₂ via acetate. Although propionate degradation to

488 acetate is thermodynamically unfavourable under standard conditions ($\Delta G^{\circ} = +76$
489 kJ/mol), hydrogenotrophic methanogenesis in the microcosms could have lowered the
490 H_2 partial pressure, providing suitable conditions for propionate conversion to acetate.
491 Similar interactions were observed in paddy soils, where *Syntrophobacter* spp were
492 found to be the dominant propionate degraders. These organisms were suggested to
493 degrade propionate in syntrophy with hydrogenotrophic methanogens in the absence
494 of sulfate, however they switch to sulfate reduction when sulfate became available (Liu
495 and Conrad, 2017).

496

497 Metabolic pathways were different in butyrate and TMA-amended incubations as
498 inferred from the bacterial and methanogenic community structures in these
499 microcosms. Results suggest that the genus *Syntrophomonas* degraded butyrate to
500 acetate. Meanwhile, members of the *Desulfarculus baarsii* lineage may have
501 completely oxidised butyrate and produced CO_2 while reducing sulfate (Figure 6c). In
502 the sulfate-free control incubations, they may have worked in syntrophy with H_2
503 oxidisers. Additionally, *Syntrophobacter* spp. likely degraded butyrate to CO_2 and H_2 .
504 Metagenomic analysis of samples from lab-scale anaerobic digesters demonstrated
505 that *Syntrophobacterales* have the metabolic potential to degrade reduced carbon
506 compounds such as butyrate and propionate to acetate, CO_2 and H_2 (Vanwonterghem
507 et al., 2016). The highest relative abundance of *Syntrophobacter* spp (12% of *dsrB*
508 sequences) was in the 0.5 COD/ SO_4^{2-} ratio microcosms compared to 4.8-8% in control
509 and higher COD/ SO_4^{2-} ratios. The high abundance of these complete-oxidisers conflicts
510 with findings of Muyzer and Stams (Muyzer and Stams, 2008), who suggested that
511 incomplete oxidisers of SRB would dominate over complete oxidisers when degrading
512 butyrate.

513

514 The increased relative abundance of the genus *Methanomethylovorans* in the TMA
515 microcosms indicates that part of the TMA was converted to methane directly via
516 methylotrophic methanogenesis (Figure 6d). Interestingly, sulfate removal was also
517 observed in these incubations although TMA has not been shown to be a growth
518 substrate for SRB previously. Interspecies H₂ transfer between *Methanomethylovorans*
519 spp. and the SRB may well have been the mechanism behind the sulfate reduction
520 observed. As demonstrated previously, when methylotrophic methanogens and
521 hydrogenotrophic SRB are in the same environment, the methanogens produce H₂,
522 which serves as the electron donor for hydrogenotrophic SRB via interspecies H₂
523 transfer (Phelps et al., 1985; Finke et al., 2007). On the other hand, *Methanobacterium*
524 spp (hydrogenotrophic methanogens) used H₂+CO₂ to generate methane. Hence,
525 together with the hydrogenotrophic SRB, they would have maintained low H₂
526 concentrations, thus facilitating the H₂ production by methylotrophic methanogens
527 (Meuer et al., 2002). Finke et al. (2007) have suggested that this H₂ loss mechanism
528 allows the methanogens to be active even when sulfate is available. Indeed, in our
529 experiments, the availability of sulfate did not affect the methanogenic diversity.
530 However, further experiments are required to confirm the metabolic interaction
531 between SRB and methylotrophic methanogens when degrading TMA.

532

533 The results of this study should be useful to develop strategies to increase the
534 methane yield from full-scale anaerobic digesters receiving sulfate-containing
535 wastewaters. For instance, a two-stage anaerobic treatment may be operated to
536 increase the acetate and propionate concentrations during the acidification step. Since
537 we have demonstrated that the COD/SO₄²⁻ ratio does not affect the methane production
538 when acetate and propionate are the carbon sources, a higher methane yield may be
539 obtained in the second reactor than when a one-reactor strategy is followed. Moreover,

540 the acidification reactor can be operated under alkaline conditions to increase the
541 propionate production when the influent is a protein-rich wastewater.

542

543 **4. CONCLUSION**

544 Our results demonstrate that in a microbial community sourced from a sulfate
545 acclimated reactor, methane production and sulfate reduction were independent
546 processes and that the COD/SO₄²⁻ ratio did not affect the microbial community
547 structure, although the presence of sulfate can result in a shift in the metabolic pathway
548 to simultaneous methanogenesis and sulfate reduction. The main factor influencing the
549 microbial community structure, and hence the metabolic pathways, was the carbon
550 source. This indicates a more important role for the substrate in anaerobic reactors
551 than merely the COD/SO₄²⁻ ratio, which was previously suggested to be the key
552 parameter.

553

554

555 **ACKNOWLEDGEMENTS**

556 We are grateful to John Weir from Jacobs Douwe Egberts Ltd. (UK) for providing
557 anaerobic sludge samples. We are also grateful to Alexander Loy (University of
558 Vienna) for sharing the primer sequences ahead of publication and help with the *dsrB*
559 database. We would like to thank Patrick K. H. Lee (City University of Hong Kong) for
560 providing the *mcrA* database and related documents for bioinformatics analysis; Chloe
561 Economou for help with the qPCR analysis and Isaac Owusu-Agyeman for
562 proofreading the manuscript. This work was supported by the British Council Newton
563 Fund Travel Grants.

564

565 **Conflict of Interest:** Authors declare no conflict of financial interest.

566

567 **REFERENCES**

- 568 Bae, H., Holmes, M.E., Chanton, J.P., Reddy, K.R., 2015. Reducing Prokaryotes in the
569 Florida Everglades 81, 7431–7442.
- 570 Bhattacharya, S.K., Uberoi, V., Dronamraju, M.M., 1996. Interaction between acetate
571 fed sulfate reducers and methanogens. *Water Res.* 30, 2239–2246.
- 572 Bolger, A.M., Lohse, M., Usadel, B., 2014. Trimmomatic: A flexible trimmer for Illumina
573 sequence data. *Bioinformatics* 30, 2114–2120.
- 574 Boone, D.R., 2001. *Methanobacterium*, in: Boone, D.R., Castenholz, R. (Eds.),
575 *Bergey's Manual of Systematic Bacteriology*. Volume 1: The Archaea and the
576 Deeply Branching and Phototrophic Bacteria. Springer, New York, N.Y., pp. 215–
577 218.
- 578 Boone, D.R., Bryant, M.P., 1980. Propionate degrading bacterium, *Syntrophobacter*
579 *wolinii* sp. nov. gen. nov., from methanogenic systems. *Appl. Environ. Microbiol.*
580 40, 626–632.
- 581 Bryant, M.P., Wolin, E.A., Wolin, M.J., Wolfe, R.S., 1967. *Methanobacillus omelianskii*,
582 a symbiotic association of two species of bacteria. *Arch. Microbiol.* 59, 20–31.
- 583 Bushwell, A.M., Mueller, H.F., 1952. Mechanism of methane fermentation. *Ind. Eng.*
584 *Chem* 44, 550–552.
- 585 Caporaso, J.G., Lauber, C.L., Walters, W.A., Berg-Lyons, D., Huntley, J., Fierer, N.,
586 Owens, S.M., Betley, J., Fraser, L., Bauer, M., Gormley, N., Gilbert, J.A., Smith,
587 G., Knight, R., 2012. Ultra-high-throughput microbial community analysis on the
588 Illumina HiSeq and MiSeq platforms. *ISME J* 6, 1621-1624.
- 589 Caporaso, J.G., Kuczynski, J., Stombaugh, J., Bittinger, K., Bushman, F.D., Costello,
590 E.K., Fierer, N., Peña, A.G., Goodrich, J.K., Gordon, J.I., Huttley, G. a, Kelley,
591 S.T., Knights, D., Koenig, J.E., Ley, R.E., Lozupone, C. a, Mcdonald, D., Muegge,
592 B.D., Pirrung, M., Reeder, J., Sevinsky, J.R., Turnbaugh, P.J., Walters, W. a,
593 Widmann, J., Yatsunenko, T., Zaneveld, J., Knight, R., 2010. QIIME allows
594 analysis of high- throughput community sequencing data Intensity normalization

595 improves color calling in SOLiD sequencing. *Nat. Methods* 7, 335–336.

596 Choi, E., Rim, J.M., 1991. Competition and Inhibition of Sulfate Reducers and Methane
597 Producers in Anaerobic Treatment. *Water Sci. Technol.* 23, 1259–1264.

598 Demirel, B., Scherer, P., 2008. The roles of acetotrophic and hydrogenotrophic
599 methanogens during anaerobic conversion of biomass to methane: A review. *Rev.*
600 *Environ. Sci. Biotechnol.* 7, 173–190.

601 DeSantis, T.Z., Hugenholtz, P., Larsen, N., Rojas, M., Brodie, E.L., Keller, K., Huber,
602 T., Dalevi, D., Hu, P., Andersen, G.L., 2006. Greengenes, a chimera-checked 16S
603 rRNA gene database and workbench compatible with ARB. *Appl. Environ.*
604 *Microbiol.* 72, 5069–5072.

605 Dolfing, J., 2014. Thermodynamic constraints on syntrophic acetate oxidation. *Appl.*
606 *Environ. Microbiol.* 80, 1539–1541.

607 Edgar, R.C., 2010. Search and clustering orders of magnitude faster than BLAST.
608 *Bioinformatics* 26, 2460–2461.

609 Finke, N., Hoehler, T.M., Jørgensen, B.B., 2007. Hydrogen “leakage” during
610 methanogenesis from methanol and methylamine: Implications for anaerobic
611 carbon degradation pathways in aquatic sediments. *Environ. Microbiol.* 9, 1060–
612 1071.

613 Haas BJ, Gevers D, Earl AM, Feldgarden M, Ward DV et al, 2011. Chimeric 16S rRNA
614 sequence formation and detection in Sanger and 454-pyrosequenced PCR
615 amplicons. *Genome Res* 21, 494-504.

616 Hammer, Ø., Harper, D.A.T. a. T., Ryan, P.D., 2001. PAST: Paleontological Statistics
617 Software Package for Education and Data Analysis. *Palaeontol. Electron.* 4(1),
618 1–9.

619 Hoeks, F., Hoopen, T.H., JA, R., JG., K., 1984. Anaerobic treatment of acid water
620 (methane production in a sulphate rich environment). *Prog Ind Microbiol* 20, 113–
621 119.

622 Hu, Y., Jing, Z., Sudo, Y., Niu, Q., Du, J., Wu, J., Li, Y.Y., 2015. Effect of influent

623 COD/SO₄²⁻ ratios on UASB treatment of a synthetic sulfate-containing
624 wastewater. *Chemosphere* 130, 24–33.

625 Ince, O., Kolukirik, M., Cetecioglu, Z., Eyice, O., Tamerler, C., Kasapgil Ince, B., 2007.
626 Methanogenic and sulphate reducing bacterial population levels in a full-scale
627 anaerobic reactor treating pulp and paper industry wastewater using fluorescence
628 in situ hybridisation. *Water Sci. Technol.* 55, 183-191.

629 Isa, Z., Grusenmeyer, S., Verstraete, W., 1986. Sulfate Reduction Relative to Methane
630 Production in High-Rate Anaerobic Digestion: Technical Aspects. *Appl. Environ.*
631 *Microbiol.* 51, 572–579.

632 King, G.M., 1984. Metabolism of trimethylamine, choline, and glycine betaine by
633 sulfate-reducing and methanogenic bacteria in marine sediments. *Appl. Environ.*
634 *Microbiol.* 48, 719–725.

635 Kiyuna, L.S.M., Fuess, L.T., Zaiat, M., 2017. Unraveling the influence of the
636 COD/sulfate ratio on organic matter removal and methane production from the
637 biodigestion of sugarcane vinasse. *Bioresour. Technol.* 232, 103–112.

638 Koornneef, J., Van Breevoort, P., Noothout, P., Hendriks, C., Luning, L., Camps, A.,
639 2013. Global potential for biomethane production with carbon capture, transport
640 and storage up to 2050. *Energy Procedia* 37, 6043–6052.

641 Lens, P.N.L., Visser, A., Janssen, A.J.H., Pol, L.W.H., Lettinga, G., 1998.
642 Biotechnological treatment of sulfate-rich wastewaters. *Crit. Rev. Environ. Sci.*
643 *Technol.* 28, 41–88.

644 Liu, P., Conrad, R., 2017. Syntrophobacteraceae-affiliated species are major
645 propionate-degrading sulfate reducers in paddy soil. *Environ. Microbiol.* 19, 1669–
646 1686.

647 Lomans, B.P., Maas, R., Luderer, R., Dencamp, H.J.M.O., Pol, A., Vanderdrift, C.,
648 Vogels, G.D., 1999. Isolation and characterization of Methanomethylovorans
649 hollandica gen. nov., sp nov., isolated from freshwater sediment, a methylotrophic.
650 *Appl. Environ. Microbiol.* 65, 3641–3650.

651 Lu, X., Zhen, G., Ni, J., Hojo, T., Kubota, K., Li, Y.Y., 2016. Effect of influent
652 COD/SO₄²⁻ ratios on biodegradation behaviors of starch wastewater in an upflow
653 anaerobic sludge blanket (UASB) reactor. *Bioresour. Technol.* 214, 175–183.

654 Maillacheruvu, K.Y., Parkin, G.F., 1996. Kinetics of growth, substrate utilization and
655 sulfide toxicity for propionate, acetate, and hydrogen utilizers in anaerobic
656 systems. *Water Environ. Res.* 68, 1099–1106.

657 Meurer, J., Kuettner, H.C., Zhang, J.K., Hedderich, R., Metcalf, W.W., 2002. Genetic
658 analysis of the archaeon *Methanosarcina barkeri* Fusaro reveals a central role for
659 Ech hydrogenase and ferredoxin in methanogenesis and carbon fixation. *Proc.*
660 *Natl. Acad. Sci.* 99, 5632–5637.

661 Müller, A.L., Kjeldsen, K.U., Rattei, T., Pester, M., Loy, A., 2015. Phylogenetic and
662 environmental diversity of DsrAB-type dissimilatory (bi)sulfite reductases. *ISME J.*
663 9, 1152–1165.

664 Müller, B., Sun, L., Schnürer, A., 2013. First insights into the syntrophic acetate-
665 oxidizing bacteria - a genetic study. *Microbiologyopen* 2, 35–53.

666 Müller, N., Worm, P., Schink, B., Stams, A.J.M., Plugge, C.M., 2010. Syntrophic
667 butyrate and propionate oxidation processes: From genomes to reaction
668 mechanisms. *Environ. Microbiol. Rep.* 2, 489–499.

669 Muyzer, G., Stams, A.J.M., 2008. The ecology and biotechnology of sulphate-reducing
670 bacteria. *Nat. Rev. Microbiol.* 6, 441–454.

671 O'Flaherty, V., Lens, P., Leahy, B., Colleran, E., 1998. Long-term competition between
672 sulphate-reducing and methane-producing bacteria during full-scale anaerobic
673 treatment of citric acid production wastewater. *Water Res.* 32, 815–825.

674 O'Reilly, C., Colleran, E., 2006. Effect of influent COD/SO₄²⁻ ratios on mesophilic
675 anaerobic reactor biomass populations: Physico-chemical and microbiological
676 properties. *FEMS Microbiol. Ecol.* 56, 141–153.

677 Oremland, R.S., Polcin, S., 1982. Methanogenesis and sulfate reduction: competitive
678 and noncompetitive substrates in estuarine sediments. *Appl. Environ. Microbiol.*

679 44, 1270–1276.

680 Parkin, G.F., Lynch, N.A., Kuo, W.C., van Keren, E.L., Bhattacharya, S.K., 1990.

681 Interaction between sulfate reducers and methanogens fed acetate and

682 propionate. Res. J. WPCF 62, 780–788.

683 Phelps, T.J., Conrad, R., Zeikus, J.G., 1985. Sulfate-dependent interspecies H₂

684 transfer between *Methanosarcina barkeri* and *Desulfovibrio vulgaris* during

685 coculture metabolism of acetate or methanol. Appl. Environ. Microbiol. 50, 589–

686 594.

687 Plugge, C.M., Zhang, W., Scholten, J.C.M., Stams, A.J.M., 2011. Metabolic flexibility of

688 sulfate-reducing bacteria. Front. Microbiol. 2, 1–8.

689 Pol, L.W.H., Lens, P.N.L., Stams, A.J.M., Lettinga, G., 1998. Anaerobic treatment of

690 sulphate-rich wastewaters. Biodegradation 9, 213–224.

691 Purdy, K.J., 2005. Nucleic acid recovery from complex environmental samples.

692 Methods Enzymol. 397, 271–292.

693 Purdy, K.J., Munson, M.A., Cresswell-Maynard, T., Nedwell, D.B., Embley, T.M.,

694 2003a. Use of 16S rRNA-targeted oligonucleotide probes to investigate function

695 and phylogeny of sulphate-reducing bacteria and methanogenic archaea in a UK

696 estuary. FEMS Microbiol. Ecol. 44, 361–371.

697 Purdy, K.J., Nedwell, D.B., Embley, T.M., 2003b. Analysis of the sulfate-reducing

698 bacterial and methanogenic archaeal populations in contrasting antarctic

699 sediments. Appl. Environ. Microbiol. 69, 3181–3191.

700 Qatibi, A.I., Boris, A., Garcia, J.L., 1990. Effect of sulfate on lactate and C₂, C₃ volatile

701 fatty acids anaerobic degradation by mixed microbial culture. Antonie Van

702 Leeuwenhoek 53, 241–248.

703 Raskin, L., Rittman, B.E., Stahl, D.A., 1996. Competition and coexistence of sulfate-

704 reducing and methanogenic populations in anaerobic biofilms. Appl. Environ.

705 Microbiol. 62, 3847–3857.

706 Schmidt, A., Müller, N., Schink, B., Schleheck, D., 2013. A Proteomic View at the

707 Biochemistry of Syntrophic Butyrate Oxidation in *Syntrophomonas wolfei*. PLoS
708 One 8(2): e56905.

709 Schmidt, O., Hink, L., Horn, M.A., Drake, H.L., 2016. Peat: Home to novel syntrophic
710 species that feed acetate- and hydrogen-scavenging methanogens. ISME J. 10,
711 1954–1966.

712 Schnürer, A., Nordberg, Å., 2008. Ammonia, a selective agent for methane production
713 by syntrophic acetate oxidation at mesophilic temperature. Water Sci. Technol.
714 57, 735–740.

715 Schönheit, P., Kristjansson, J.K., Thauer, R.K., 1982. Kinetic mechanism for the ability
716 of sulfate reducers to outcompete methanogens for acetate. Arch. Microbiol. 132,
717 285–288.

718 Sobieraj, M., Boone, D.R., 2006. Syntrophomonadaceae, in: The Prokaryotes. pp.
719 1041–1049.

720 Sousa, D.Z., Smidt, H., Alves, M.M., Stams, A.J.M., 2007. *Syntrophomonas zehnderi*
721 sp nov., an anaerobe that degrades long-chain fatty acids in co-culture with
722 *Methanobacterium formicicum*. Int. J. Syst. Evol. Microbiol. 57, 609–615.

723 Stams, A.J.M., Plugge, C.M., 2009. Electron transfer in syntrophic communities of
724 anaerobic bacteria and archaea. Nat. Rev. Microbiol. 7, 568–577.

725 Sun, H., Spring, S., Lapidus, A., Davenport, K., del Rio, T.G., Tice, H., Nolan, M.,
726 Copeland, A., Cheng, J.F., Lucas, S., Tapia, R., Goodwin, L., Pitluck, S., Ivanova,
727 N., Pagani, I., Mavromatis, K., Ovchinnikova, G., Pati, A., Chen, A., Palaniappan,
728 K., Hauser, L., Chang, Y.J., Jeffries, C.D., Detter, J.C., Han, C., Rohde, M.,
729 Brambilla, E., Göker, M., Woyke, T., Bristow, J., Eisen, J.A., Markowitz, V.,
730 Hugenholtz, P., Kyrpides, N.C., Klenk, H.P., Land, M., 2010. Complete genome
731 sequence of *Desulfarculus baarsii* type strain (2st14T). Stand. Genomic Sci. 3,
732 276–284.

733 Ueki, K., Ueki, A., Takahashi, K., Iwatsu, M., 1992. The Role of Sulfate Reduction in
734 Methanogenic Digestion of Municipal Sewage Sludge. J. Gen. Appl. Microbiol. 38,

735 195–207.

736 Vanwonterghem, I., Jensen, P.D., Rabaey, K., Tyson, G.W., 2016. Genome-centric
737 resolution of microbial diversity, metabolism and interactions in anaerobic
738 digestion. *Environ. Microbiol.* 18, 3144–3158.

739 Vich, D., Garcia, M., Varesche, M., 2011. Methanogenic potential and microbial
740 community of anaerobic batch reactors at different methylamine/sulfate ratios.
741 *Brazilian J. Chem. Eng.* 28, 1–8.

742 Wang, Q., Garrity, G.M., Tiedje, J.M., Cole, J.R., 2007. Naïve Bayesian classifier for
743 rapid assignment of rRNA sequences into the new bacterial taxonomy. *Appl.*
744 *Environ. Microbiol.* 73, 5261–5267.

745 WBA, 2014. WBA Global Bioenergy Statistics 2014. World Bioenergy Assoc. 40.

746 Werner, J.J., Knights, D., Garcia, M.L., Scalfone, N.B., Smith, S., Yarasheski, K.,
747 Cummings, T.A., Beers, A.R., Knight, R., Angenent, L.T., 2011. Bacterial
748 community structures are unique and resilient in full-scale bioenergy systems.
749 *Proc. Natl. Acad. Sci.* 108, 4158–4163.

750 Wilkins, D., Lu, X.Y., Shen, Z., Chen, J., Lee, P.K.H., 2015. Pyrosequencing of *mcrA*
751 and archaeal 16S rRNA genes reveals diversity and substrate preferences of
752 methanogen communities in anaerobic digesters. *Appl. Environ. Microbiol.* 81,
753 604–613.

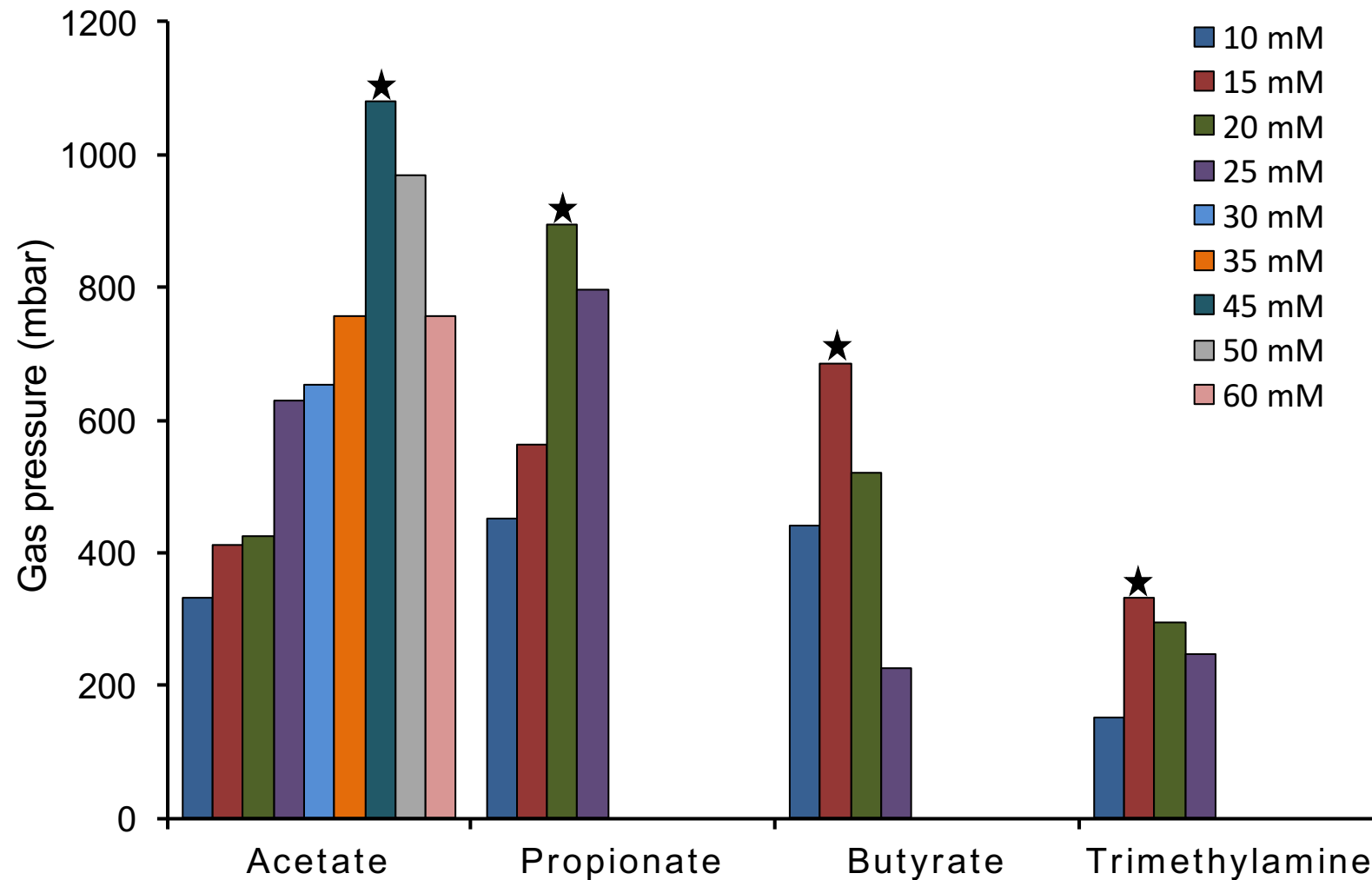
754 Yang, S.L., Tang, Y.Q., Gou, M., Jiang, X., 2015. Effect of sulfate addition on methane
755 production and sulfate reduction in a mesophilic acetate-fed anaerobic reactor.
756 *Appl. Microbiol. Biotechnol.* 99, 3269–3277.

757

**COD/sulfate ratio does not affect the methane yield and
microbial diversity in anaerobic digesters**

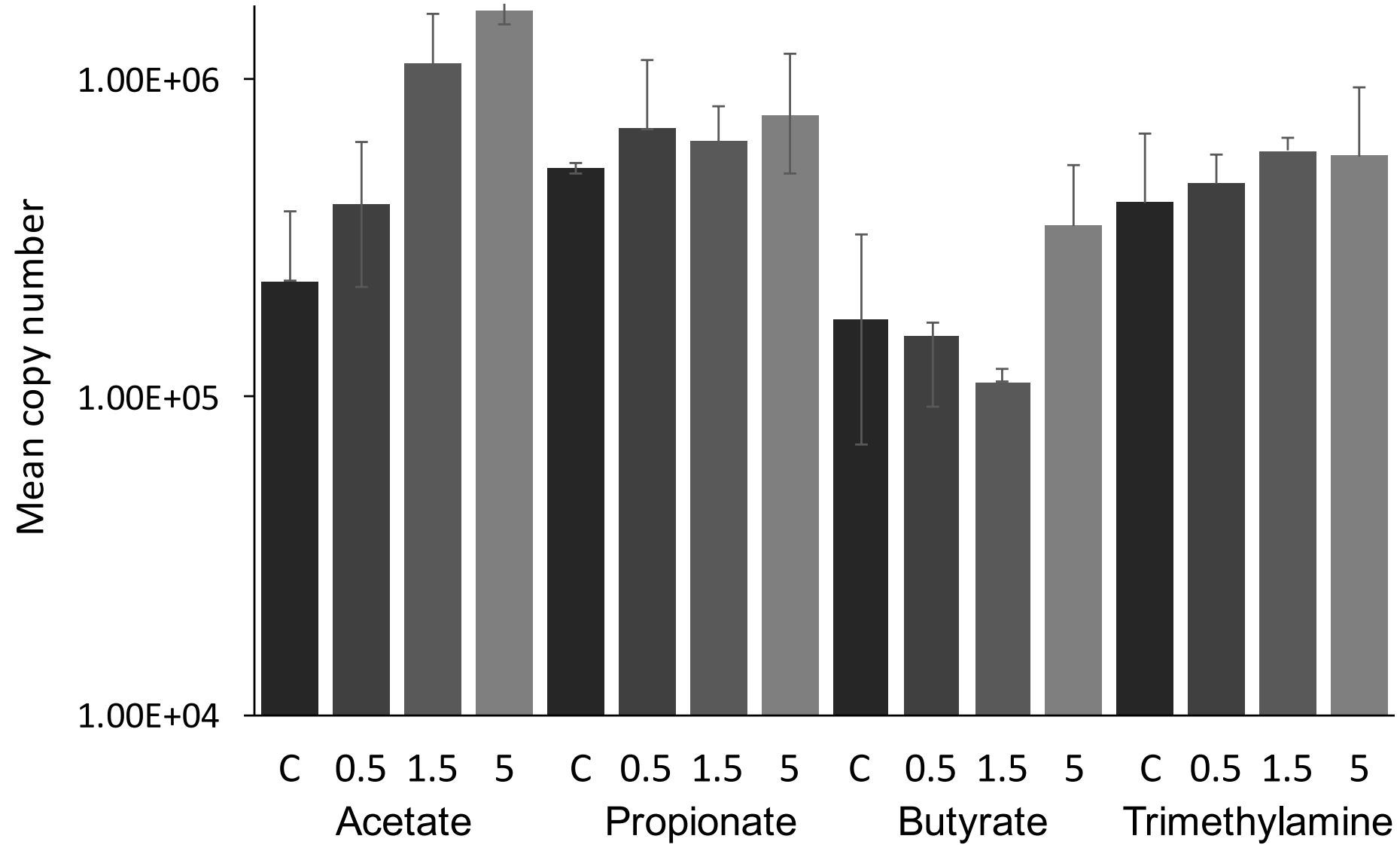
Cetecioglu et al.

Supplementary Figures and Tables



Supplementary Figure 1. Biogas production during the specific methanogenic activity tests. Maximum gas production occurred at 45 mM acetate, 20 mM propionate, 15 mM butyrate or trimethylamine.

mcrA gene abundance



Supplementary Figure 2. Abundance of the *mcrA* gene in the incubations.

Supplementary Table 1. Experimental conditions used to set up the incubations.

Carbon source	Incubation	Substrate added (mM)	Sulfate added (mM)
Acetate	Control	45	0
	COD/SO4 = 0.5	45	59.7
	COD/SO4 = 1.5	45	19.9
	COD/SO4 = 5	45	5.9
Propionate	Control	20	0
	COD/SO4 = 0.5	20	46.5
	COD/SO4 = 1.5	20	15.5
	COD/SO4 = 5	20	4.6
Butyrate	Control	15	0
	COD/SO4 = 0.5	15	66.7
	COD/SO4 = 1.5	15	22.2
	COD/SO4 = 5	15	6.67
Trimethylamine	Control	15	0
	COD/SO4 = 0.5	15	15
	COD/SO4 = 1.5	15	5
	COD/SO4 = 5	15	1.5

Supplementary Table 2. Primers used in this study.

Target gene	Primer name	Sequence (5'-3')	Reference
16S rRNA Bacteria	515F	GTGCCAGCMGCCGCGGTAA	Caporaso et al., 2011
	806R	GGACTACHVGGGTWTCTAAT	
16S rRNA Archaea	Parch519F	CAGCCGCCGCGGTAA	Øvreås et al., 1997
	ARC915R	GTGCTCCCCCGCCAATTCCT	Stahl and Amann, 1991
dsrB	DSR1762Fmix	see Ref.	Pelikan et al., 2016
	DSR2107Rmix		
mcrA	mcrIRD -F	TWYGACCARATMTGGYT	Lever and Teske, 2015
	mcrIRD -R	ACRTTCATBGCRTARTT	

Supplementary Table 3. Alpha diversity indices calculated for each sample.
 C: No-sulfate control. 0.5, 1,5 and 5 represent COD/SO₄²⁻ ratios.

		Acetate				Propionate				Butyrate				TMA			
		C	0.5	1.5	5	C	0.5	1.5	5	C	0.5	1.5	5	C	0.5	1.5	5
Bacteria	OTU number	1070	1083	1016	1043	985	978	978	1029	926	880	953	884	1024	959	948	932
	Shannon's index	4.27	4.29	4.35	4.36	4.18	4.27	4.10	4.35	4.21	4.13	4.18	4.16	4.31	4.25	4.26	4.22
	Chao1	1362	1259	1186	1217	1221	1221	1173	1234	1149	1111	1209	1079	1213	1147	1121	1109
Archaea	OTU number	528	482	502	505	500	484	510	516	474	448	458	452	476	478	492	455
	Shannon's index	3.07	3.13	2.81	2.95	2.83	3.02	3.06	2.92	2.77	2.91	2.79	2.89	2.93	2.93	3.13	2.96
	Chao1	581	529	522.0	525	519	529	546	538	505	534	503	515	525	515	534	493
<i>dsrB</i>	OTU number	247	253	239	256	238	245	258	254	259	259	259	251	258	255	232	230
	Shannon's index	2.44	2.63	2.42	2.41	2.35	2.26	2.50	2.53	2.69	3.27	3.03	3.11	2.60	2.69	2.47	2.24
	Chao1	267	263	255	269	271	272	300	259	269	274	275	277	289	281	262	245
<i>mcrA</i>	OTU number	45	61	58	56	42	43	54	45	61	59	53	44	43	43	43	43
	Shannon's index	1.72	1.51	1.45	1.48	1.94	1.62	1.73	1.35	1.73	1.75	1.77	1.63	1.97	1.85	1.60	1.78
	Chao1	46	61	62	63	42	43	57	48	61	60	55	44	43	43	43	43

References

Caporaso JG, Lauber CL, Walters WA, Berg-Lyons D, Lozupone CA, Turnbaugh PJ, Fiere, N and Knight R. Global patterns of 16S rRNA diversity at a depth of millions of sequences per sample. 2011. Proc Natl Acad Sci USA. 108(1):4516-22.

Øvreås L, Forney L, Daae FL, Torsvik V. Distribution of bacterioplankton in meromictic Lake Saelenvannet, as determined by denaturing gradient gel electrophoresis of PCR-amplified gene fragments coding for 16S rRNA. 1997. Appl Environ Microbiol. 63(9):3367-73.

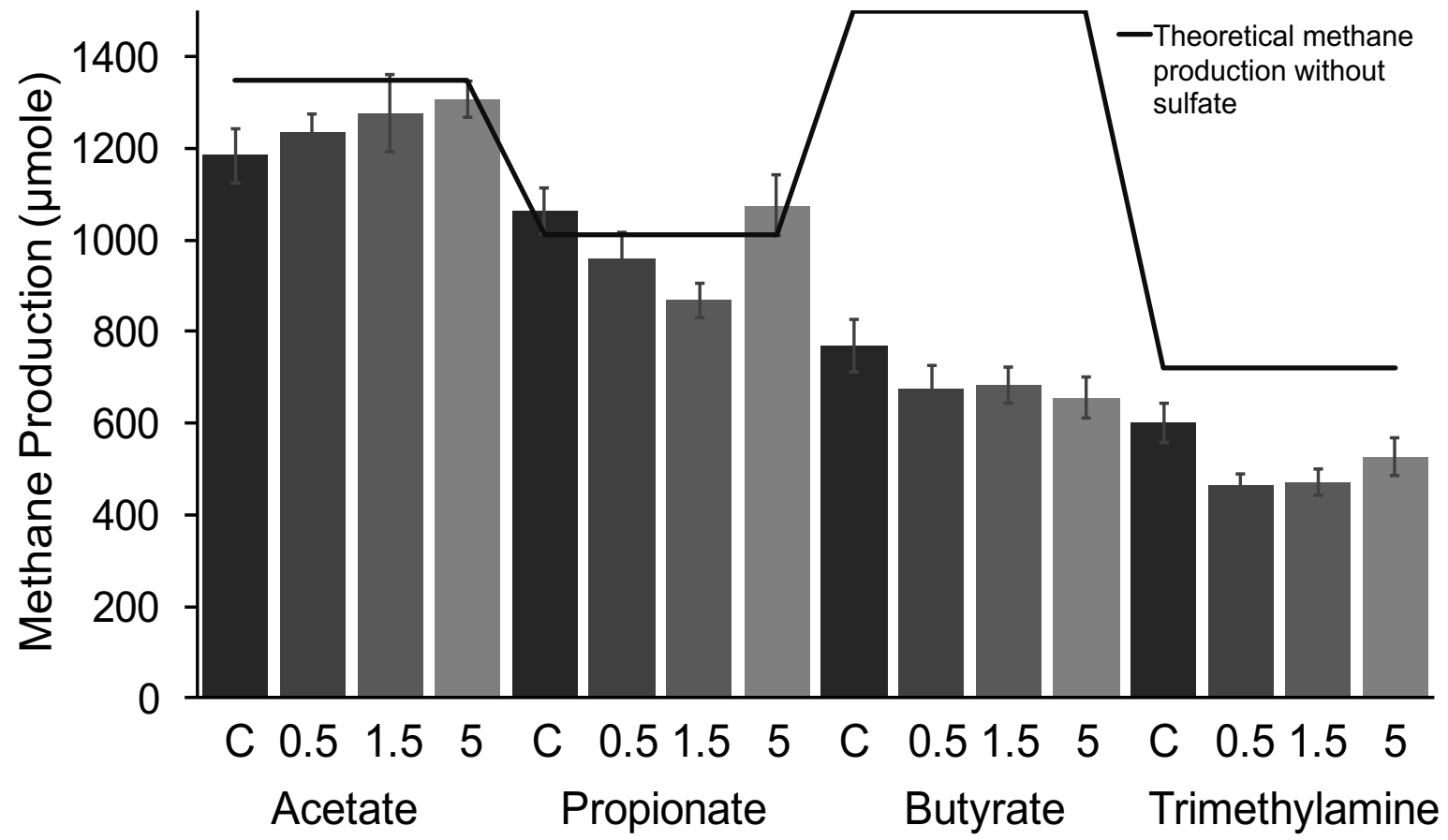
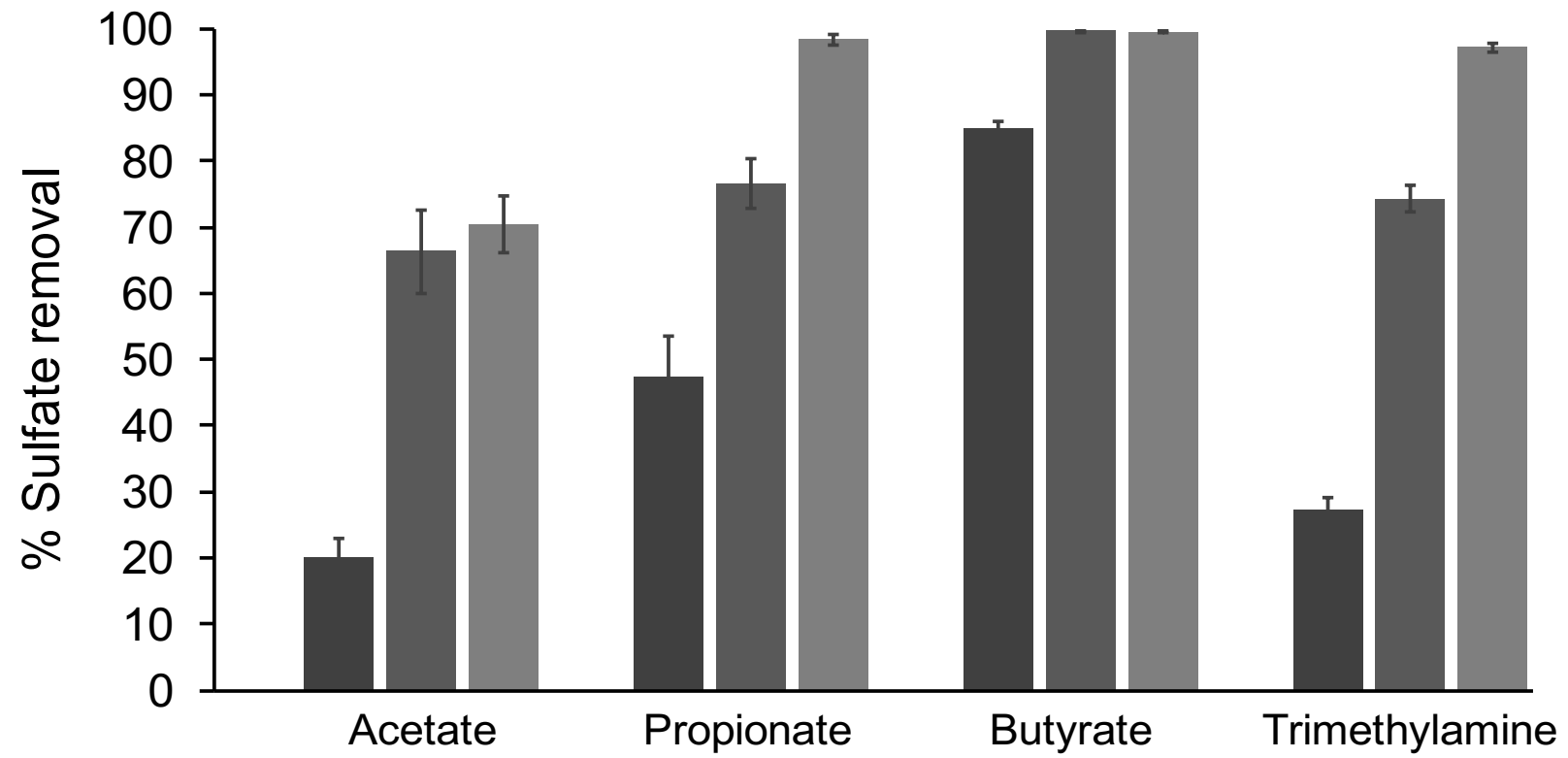
Pelikan C, Herbold CW, Hausmann B, Muller AL, Pester M, Loy A. Diversity analysis of sulfite- and sulfate-reducing microorganisms by multiplex dsrA and dsrB amplicon sequencing using new primers and mock community-optimized bioinformatics. 2016. Environ Microbiol. 18(9):2994-3009.

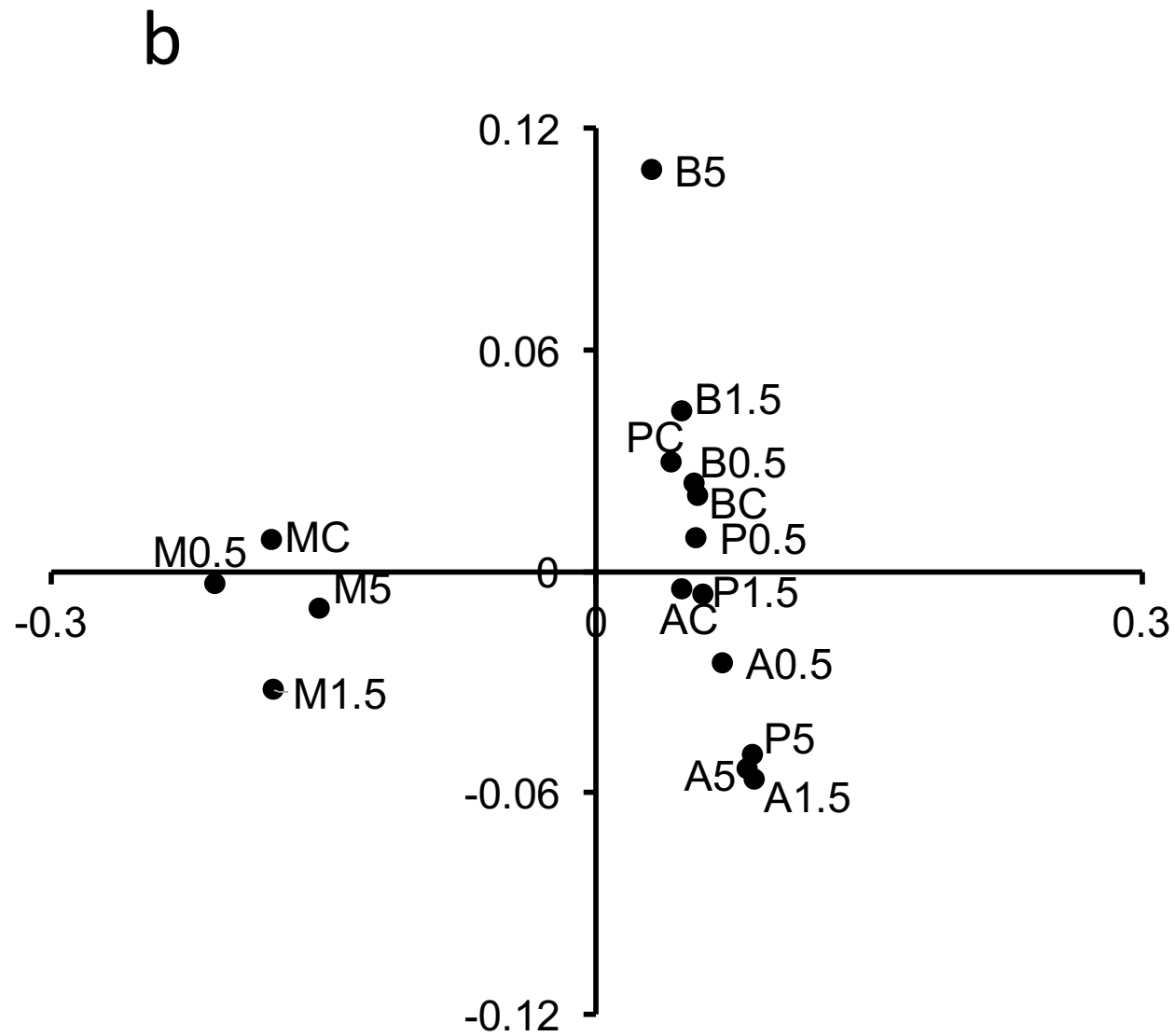
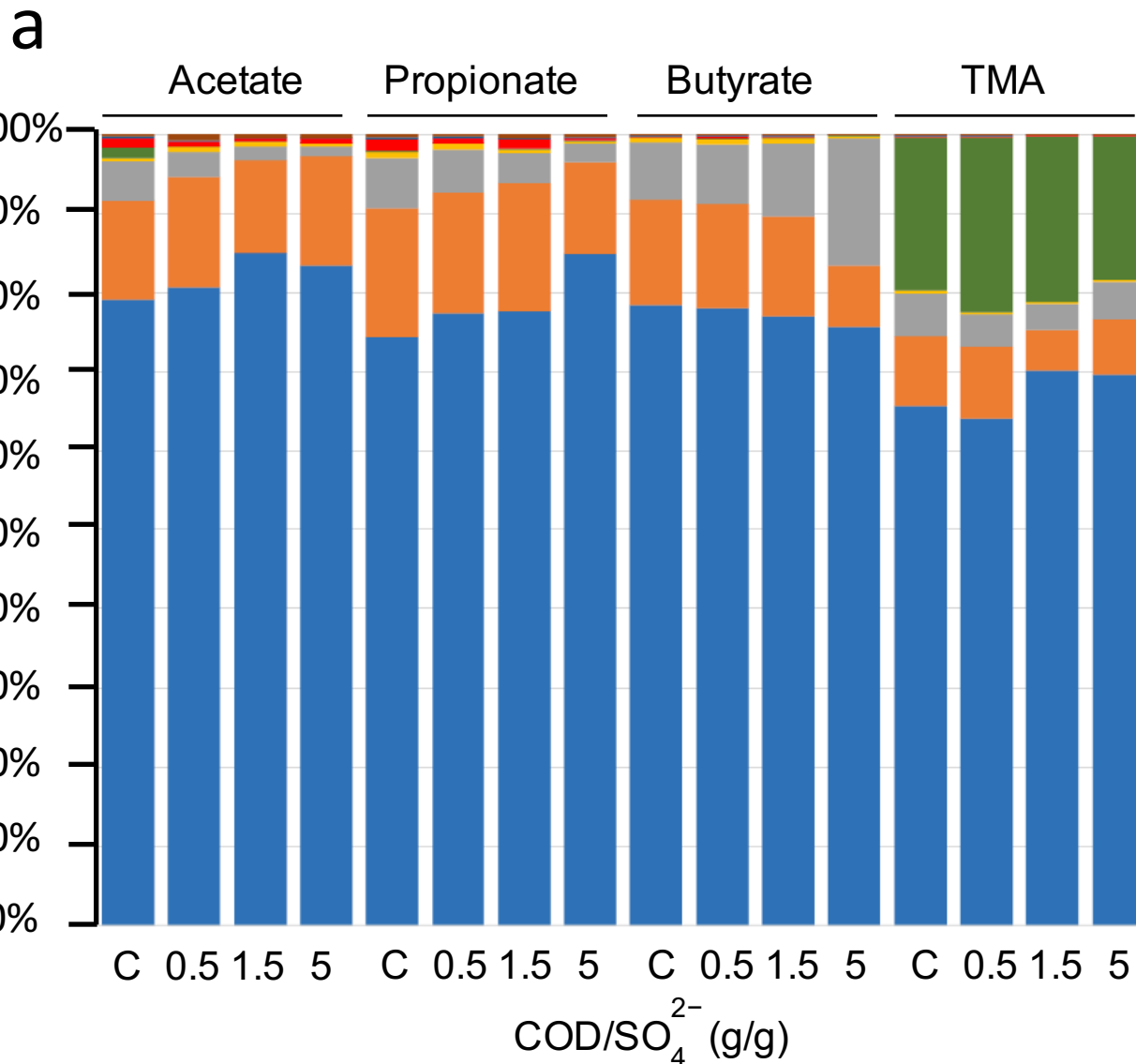
Lever MA, Teske, AP. Diversity of methane-cycling archaea in hydrothermal sediment investigated by general and group-specific PCR primers. 2015. Appl Environ Microbiol. 81(4):1426-41.

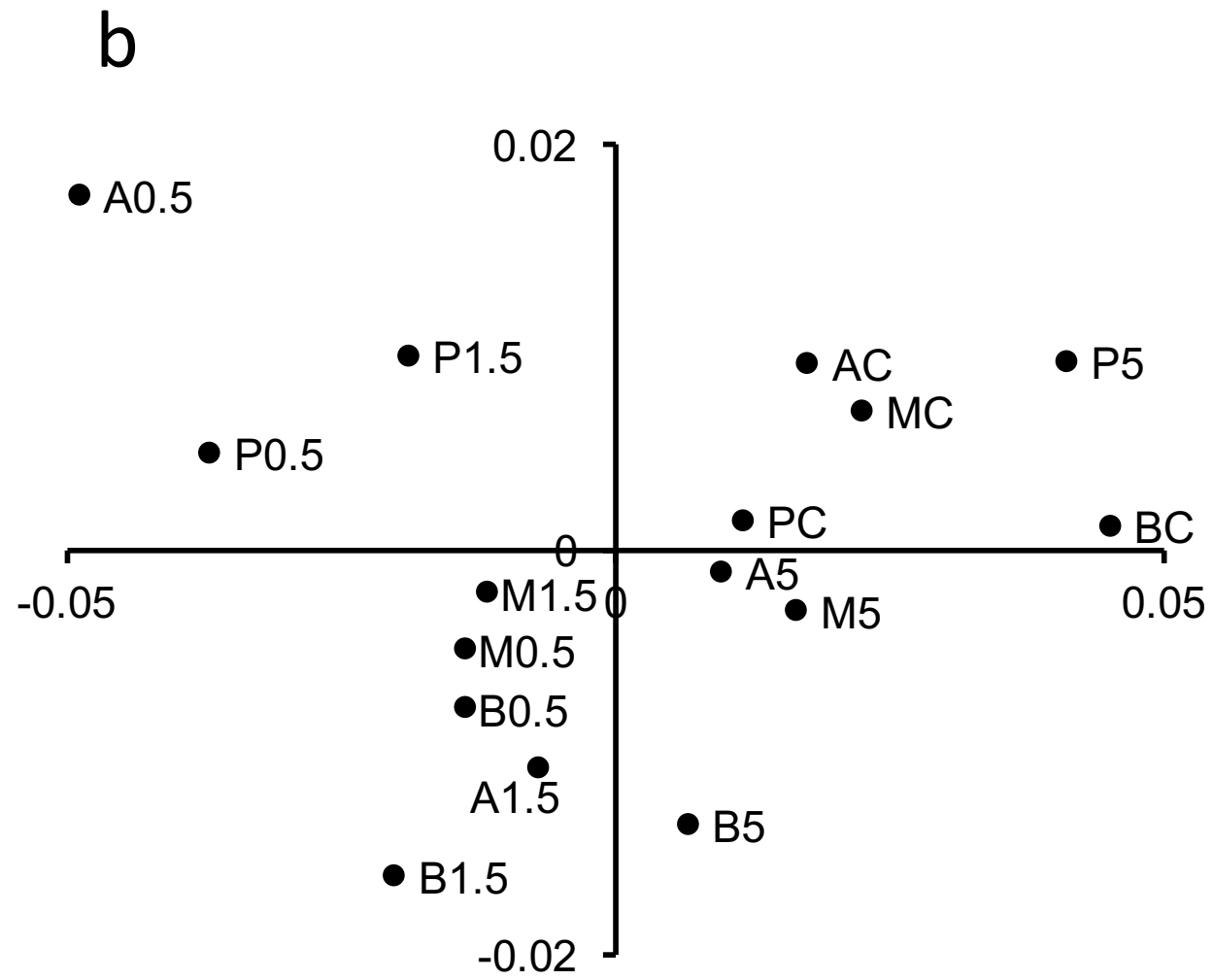
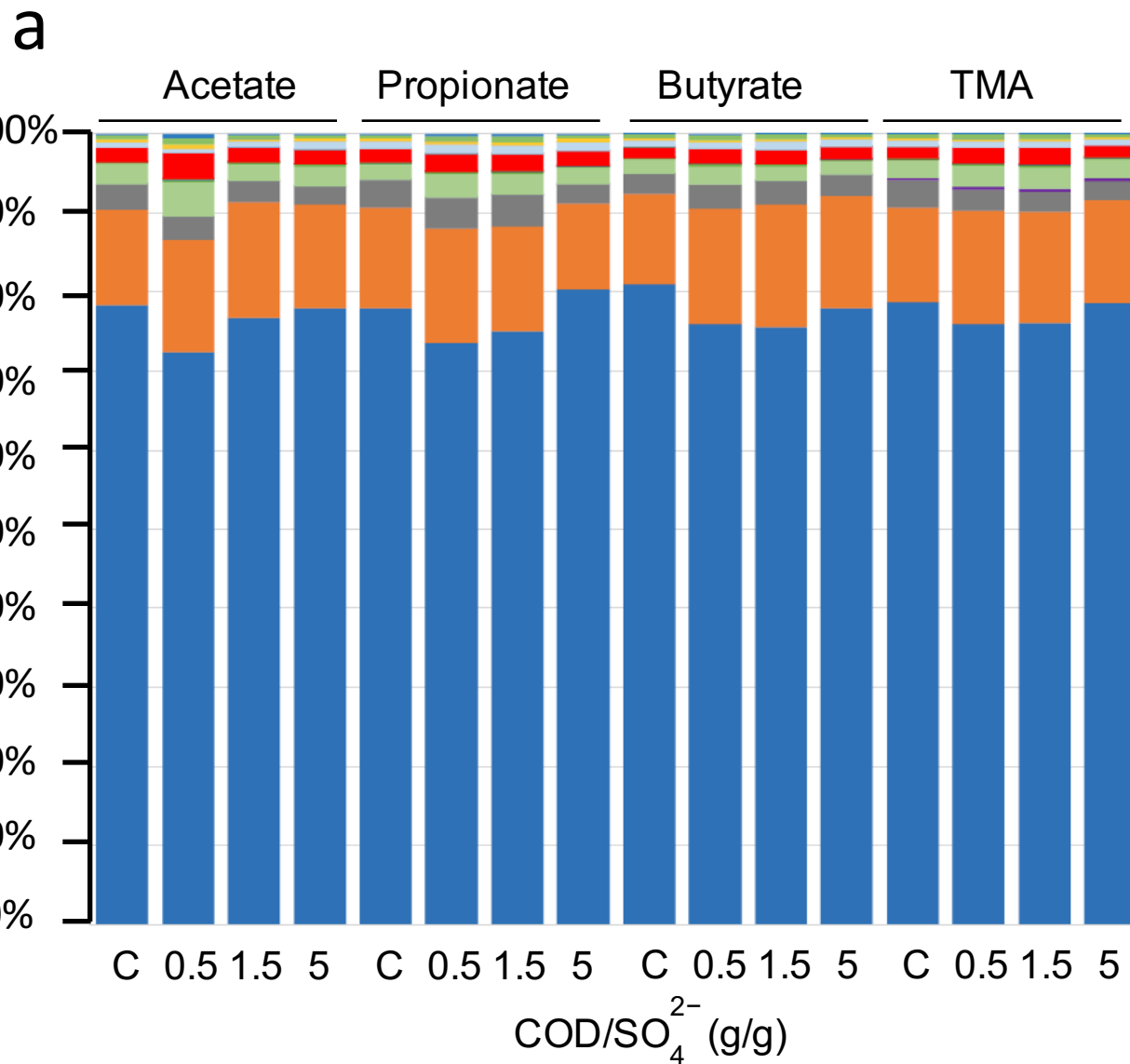
Table 1.

	Treatment	Substrate			Methane yield			Sulfate		
		Added	Residual μmol	Consumed	Actual μmol	Theoretical μmol	%	Added	Consumed μmol	%
Acetate 45 mM	Control	1350	0	1350	1184±117	1350	88	0	0	--
	COD/SO ₄ ²⁻ = 0.5	1350	0	1350	1237±73	1350	92	1792	358	20±6
	COD/SO ₄ ²⁻ = 1.5	1350	0	1350	1276±169	1350	95	597	377	66±16
	COD/SO ₄ ²⁻ = 5	1350	0	1350	1307±78	1350	97	179	126	70±9
Propionate 20 mM	Control	600	0	600	1164±99	1050	111	0	0	--
	COD/SO ₄ ²⁻ = 0.5	600	0	600	961±118	1050	92	1397	662	47±12
	COD/SO ₄ ²⁻ = 1.5	600	0	600	869±74	1050	83	466	357	77±7
	COD/SO ₄ ²⁻ = 5	600	0	600	1214±167	1050	116	140	138	99±1
Butyrate 15 mM	Control	600	0	600	770±117	1500	51	0	0	--
	COD/SO ₄ ²⁻ = 0.5	600	0	600	677±98	1500	45	2002	1694	84±2
	COD/SO ₄ ²⁻ = 1.5	600	0	600	683±76	1500	46	667	665	99±0.2
	COD/SO ₄ ²⁻ = 5	600	0	600	656±90	1500	44	200	199	99±0.2
TMA 15 mM	Control	450	123	327	602±83	734*	83	0	0	--
	COD/SO ₄ ²⁻ = 0.5	450	137	313	466±43	704*	66	451	112	25±4
	COD/SO ₄ ²⁻ = 1.5	450	130	220	473±58	720*	66	150	113	74±4
	COD/SO ₄ ²⁻ = 5	450	127	323	527±79	727*	73	45	44	98±1

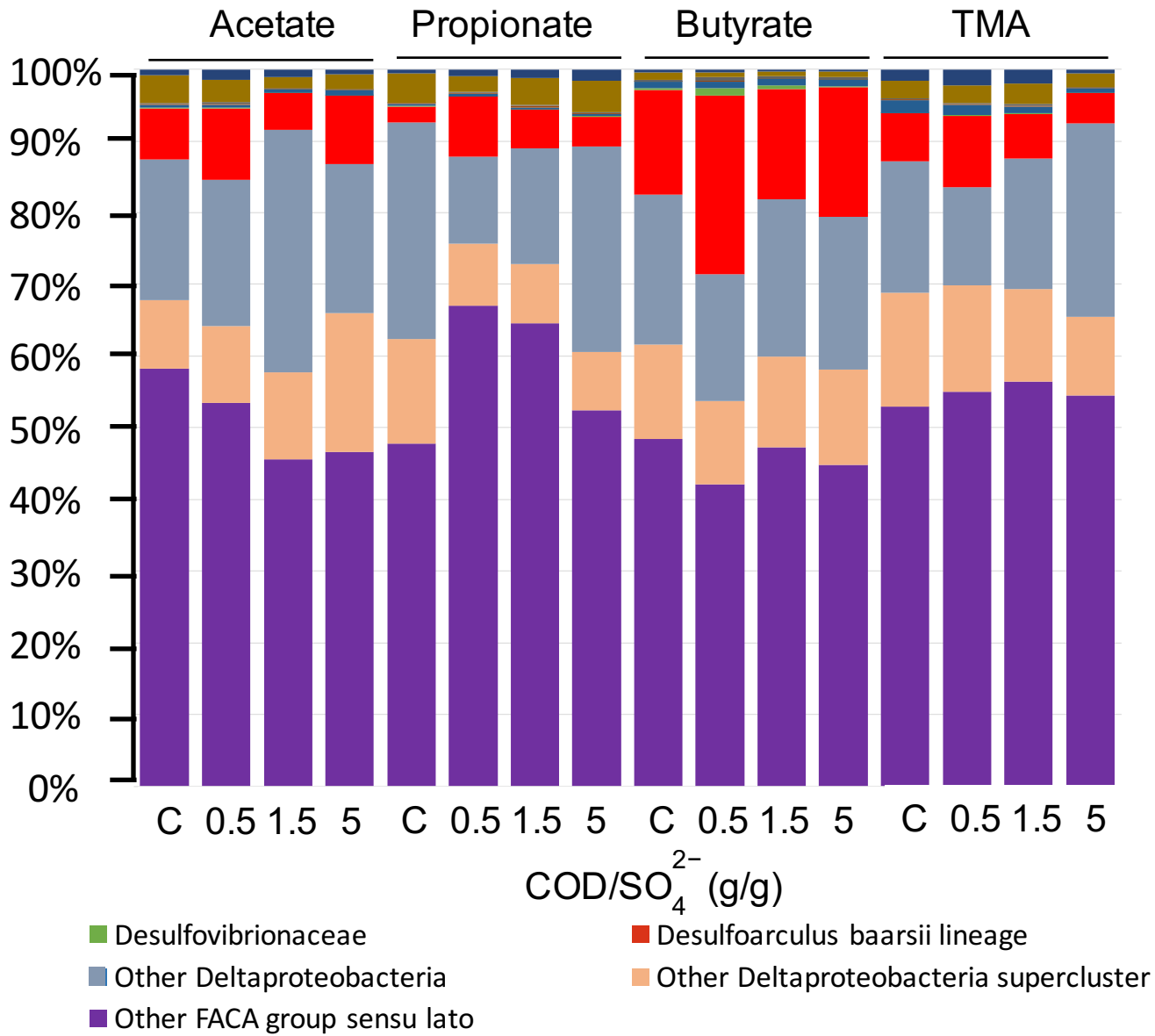
*TMA theoretical methane yield for 450 μmols of substrate was 1012.5 μmols, actual theoretical is based on total TMA consumed (70-73% of the calculated yield).

a**b**





a



b

